ENVIRONMENTAL RESEARCH
LETTERS

OPEN ACCESS

Can we control El Niño?

To cite this article: Douglas G MacMynowski 2009 *Environ. Res. Lett.* **4** 045111

Environ. Res. Lett. **4** (2009) 045111 (6pp) doi:10.1088/1748-9326/4/4/045111

Can we control El Niño?

Douglas G MacMynowski

Control and Dynamical Systems, California Institute of Technology, USA

E-mail: macmardg@cds.caltech.edu

Received 21 May 2009
Accepted for publication 24 November 2009
Published 18 December 2009
Online at stacks.iop.org/ERL/4/045111

Abstract
The question of whether it is possible to intentionally modify the El Niño/Southern oscillation (ENSO) cycle is explored as a case study in the *dynamics* of climate intervention beyond simple temperature adjustment. A plausible control strategy is described, including an estimate of the energy it would require to implement. The intent here is not to suggest that we should do so, but rather that the scale of the required intervention is such that we could intentionally influence ENSO. Simulations use the Cane–Zebiak intermediate complexity model, and demonstrate that depending on the parameter regime, a feedback strategy that dynamically deflects less than 1% of the sunlight over the Niño-3 region of the eastern tropical Pacific could be used to reduce the probability of extreme ENSO events ($T > 2\,^{\circ}$C) to near zero, or conversely to enhance the cycle.

Keywords: geoengineering, climate control, El Niño

1. Introduction

This case study begins to explore the dynamic aspects of intervention in the climate as part of a broader discussion on geoengineering (e.g. Schneider 1996, Keith 2000). There are several reasons beyond curiosity for exploring whether it is possible to 'control' El Niño; that is, to intentionally modify its dynamic evolution. First, by demonstrating a plausible approach, we gain a better understanding for the scale of influence required. This does not need to be large; a key observation is that systems which are near instability (and potentially chaotic) are extremely sensitive to small perturbations and therefore require very small control inputs. In the case of El Niño, this sensitivity can be exploited even with a relatively simple control algorithm that does not require an extremely accurate model of the system dynamics. Second, if the El Niño/Southern oscillation (ENSO) cycle changes in intensity with climate change (which is not yet clear (Cane 2005, Yeh *et al* 2009)), then a compensating strategy may be worth considering. Natural and human ecosystems have evolved in the presence of ENSO, and would experience consequences from either more extreme events, or from reduced variability. Finally, understanding how to control a system often provides a useful perspective from which to better understand the system's dynamics, such as the sensitivity of the system to small changes in natural feedback mechanisms.

In addition to understanding the physical mechanism used to influence the system, successful feedback modification of any dynamic phenomenon requires a model of the system. This paper demonstrates that it is possible to modify ENSO dynamics with a simple and robust control strategy that does not require a highly accurate dynamic model. Smaller control inputs would be needed if an optimal strategy were used, but at the expense of requiring increased knowledge about the dynamics. Note that the presence of chaotic dynamics in climate/weather phenomena does not mean that such systems are uncontrollable, indeed it improves leverage as small perturbations can lead to large changes in the response. This has been discussed in the context of weather control (Hoffman 2002), and an algorithm has been described for chaotic ENSO dynamics (Tziperman *et al* 1997). Improvements in models and observations thus translate into greater leverage for control.

Key to the question of controllability is an exploration of energetics. The dominant source of stored energy that leads to an El Niño event is the available potential energy (APE) from the slope of the tropical Pacific thermocline (Goddard and Philander 2000, Fedorov 2007, Brown and Fedorov 2008). The variation of APE in the eastern tropical Pacific over an El Niño event is of order 10^{18} J, with a peak rate of change of order 100 GW (see section 2). The mean APE is sustained by 0.2–0.4 TW mean power from the atmospheric wind stress (Brown

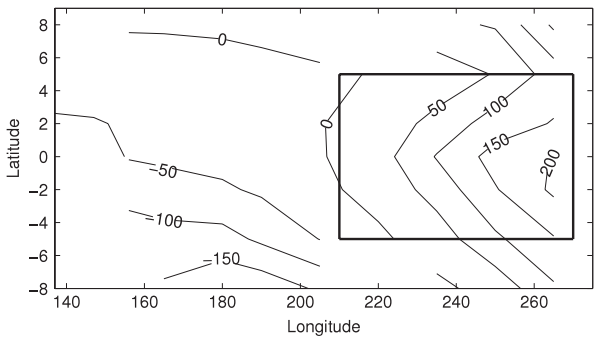

Figure 1. Mean distribution of available potential energy in the tropical Pacific, in kJ m^{-2}, computed from TAO data. The Niño-3 region is boxed.

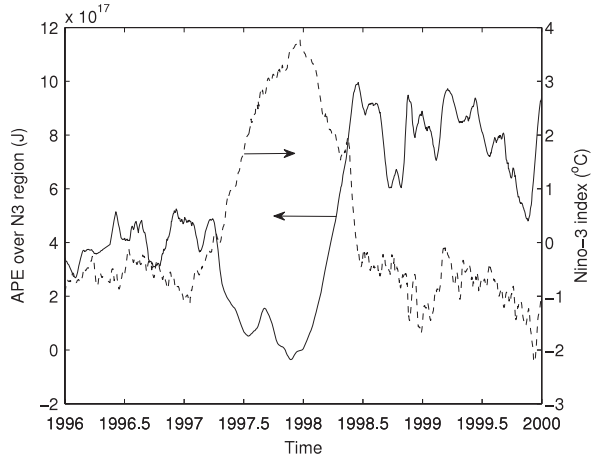

Figure 2. APE averaged over the Niño-3 region (solid curve, left-hand axis), and Niño-3 index (dashed, right-hand axis). The maximum APE gradient is roughly 100 GW.

and Fedorov 2008). To put this in context, this is roughly 0.01% of the solar radiation absorbed over the Niño-3 region.

In principle, the dynamics of ENSO could be influenced through modulation of ocean currents, atmospheric winds, or sea surface temperature (SST). These are in increasing order in terms of the power required, due to the efficiencies involved in influencing the stored APE. Nonetheless, we choose the last of these, because although this will require the greatest modulation of power, a plausible mechanism for doing so has already been suggested in the form of cloud-brightening to enhance albedo to mitigate anthropogenic climate change (Latham 2002, Latham *et al* 2008). A linearized approximation to the optimal spatial distribution of input forcing is computed herein, concluding that the sensitivity of ENSO to perturbations in absorbed solar radiation is highest in the eastern Pacific. Forcing is therefore applied uniformly over the eastern half of the Niño-3 region.

The forcing uses feedback from the Niño-3 index. The addition of feedforward information from the western-Pacific Kelvin wave amplitude is also explored. The combined control approach is demonstrated on the Zebiak and Cane (1987 hereafter ZC) intermediate complexity ENSO model. With modifications to allow data assimilation, this model has been successfully used in predicting El Niño evolution (Chen *et al* 2004). With the original parameters in the ZC model, the ENSO oscillation is chaotic (Tziperman *et al* 1994). However, there is evidence suggesting that the actual ocean physics are more likely to be stable and driven by noise (Penland and Sardeshmukh 1995, Philander and Fedorov 2003). Simulations in section 4 are shown for both regimes. While no model can ever capture the full complexity of the real world, in either case the model predictions illustrate the potential for relatively small amplitude forcing to alter the dynamic evolution of the ENSO cycle. Note that the change in ENSO amplitude is a dynamic effect; it would take much more significant energy to partially cancel or reinforce an individual event, but since there is a dynamic (memory) aspect to the ENSO cycle, smaller energy can be used to gradually damp or enhance the oscillation over time.

Section 2 summarizes the energy in the tropical Pacific, and the energy required to influence the dynamics. Section 3 describes the control approach, and section 4 gives simulation results with the Cane–Zebiak model.

2. ENSO energetics

Key to the question of what can be done with control is a consideration of the energy in El Niño and the power required to affect its evolution. It is the variation in the available potential energy (APE) associated with the thermocline slope that is dominant (Goddard and Philander 2000), rather than changes in the ocean kinetic energy. For a shallow water model, the energy per unit surface area is

$$\mathrm{APE} = \tfrac{1}{2}\rho_0 g_{\mathrm{red}}|h|h \qquad (1)$$

where h is the depth displacement relative to its mean (over the basin and over time), g_{red} is the reduced gravity and ρ_0 the density. Figure 1 plots the mean distribution of APE computed from the TAO array (McPhaden *et al* 1998) using data from 1993 to 2009, and using the approximation in equation (1) with the 20 °C isotherm as the layer depth. The variation in energy over the Niño-3 region (±5° latitude, 150°W–90°W) over the course of the 1998 El Niño event is of order 10^{18} J (roughly ∼130 kJ m^{-2}); see figure 2. The maximum power flow into or out of this region is roughly 100 GW. The energy accumulated over several years can be discharged over ∼6 months, and this thus provides an upper bound on the work required to modify ENSO dynamics through ocean forcing.

Brown and Fedorov (2008) estimate a mean of 0.2–0.4 TW wind power being transferred to the ocean over the tropical Pacific, of which 10–20% is converted into APE. Thus perturbations in wind affect the stored energy with an efficiency less than one, and thus modulating atmospheric wind will involve several times the power that directly modulating ocean currents would require. Modulating solar heating over part of the ocean will affect SST, which affects the winds, but again the changes in power will be larger than the changes in wind power that result. While this would argue for directly influencing ocean currents as the most efficient mechanism for influencing ENSO (requiring power bounded at most by 100 GW), modulating incoming solar radiation is a more plausible forcing mechanism, as noted earlier. To achieve

a given change in SST over area A, the required power is estimated as

$$Q = (C_p \rho H A)\Delta T \tag{2}$$

where H is the thickness of the surface mixed layer, obtained from de Boyer Montégut *et al* (2004). (The mean over the eastern half of the Niño-3 region is 28 m.) Q can be normalized by the mean surface solar insolation, roughly 250 W m^{-2}. The modelling herein applies the temperature perturbations ΔT directly, and computes the required change in insolation using (2); in the process, the seasonal variation in mixed layer depth and solar insolation is ignored to simplify the scaling.

In order to understand the energetics further, a brief summary of the delayed-oscillator description (Suarez and Schopf 1988) is useful, illustrated in figure 3 or by the equation

$$\dot{T} = \alpha T - \beta T(t - \delta). \tag{3}$$

While clearly incomplete in describing the evolution of an individual event, the delayed-oscillator paradigm does provide insight into the processes involved in determining ENSOs period in both data and models (Van Oldenborgh *et al* 1999, Boulanger and Menkes 1999). An SST perturbation (for example) changes the wind, which excites oceanic Kelvin and Rossby waves. The former changes the eastern-Pacific thermocline depth, which amplifies the SST perturbation through the impact on upwelling cold water. The Rossby waves propagate westward, reflect off the western boundary as a Kelvin wave, and counteract the original anomaly. However, because of the delayed effect, there is additional counteracting energy stored in the system (in the form of APE due to the thermocline anomaly); this tends to push the system towards the opposite phase of the cycle. This description leads to an oscillation that can either be stable or unstable depending on the parameters and damping. In the former case, the irregular behaviour is the result of stochastic forcing, while in the latter, self-sustained irregular behaviour can arise from (nonlinear) chaotic dynamics. In either case, a rough approximation is that the amplitude of control needs to be large enough to cancel whatever stochastic forcing exists; in the unstable regime this can be very small relative to the amplitude of the oscillation.

3. Control

For a specified location of control forcing, a (locally) optimal control input signal can be obtained by iteratively solving forward and adjoint simulations (Bewley *et al* 2001, Wei and Freund 2006), and a closed-loop control strategy obtained by embedding this in a receding-horizon control framework (Bewley *et al* 2001, Joe *et al* 2009), much as a computer plays chess by looking ahead a given number of moves. The adjoint simulations give the gradient of any chosen performance metric to changes in the control time history; the receding-horizon framework allows the forward and adjoint simulations to be done over finite time, while incorporating new measurement information as it becomes available. This is the only way in a high-dimensional chaotic system to find the 'butterfly', the flapping of whose wings can alter the trajectory of the system with negligible input (e.g. Hoffman 2002). However, this also

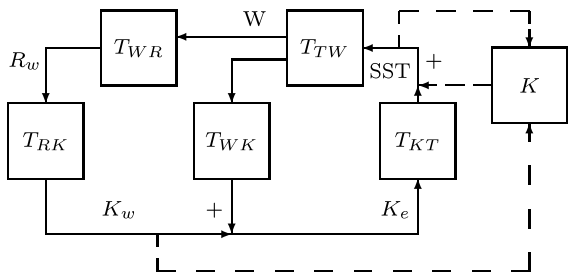

Figure 3. Schematic of ENSO delayed-oscillator physics and control K. Stochastic forcing may occur at every step but is not explicitly indicated. The right-hand feedback loop represents the eastern-Pacific physics where SST anomalies lead to changes in wind which excite Kelvin waves in the east. The left-hand feedback loop represents the delayed effect including excitation of Rossby waves, reflection off the western boundary, to create a Kelvin wave in the west. The flow of information for the control added here is shown with dashed lines.

leads to a highly model-dependent control strategy that is not likely to be robust to uncertainties. Because some fraction of the underlying dynamics of ENSO are relatively low order (giving a peak in the temporal spectrum), then with the right choice of input and output variables, we can get close to the optimal behaviour with a simpler control strategy.

We know from the physics of ENSO that SST perturbations in the eastern Pacific are highly effective, through the system dynamics, in changing future SST perturbations here. Based on the spatial distribution of forcing effectiveness (section 4), only the eastern half of the Niño-3 area is forced in the simulations. For feedback, we measure the variable we are interested in, the Niño-3 index. This gives a roughly collocated input/output system for which it is much more straightforward to develop robust control strategies that do not depend on the uncertain details of the model. A negative feedback between these variables reduces the strength of the positive feedback in the eastern Pacific, adding damping to the system. (This can also be seen by solving the eigenvalue problem associated with (3) with both α and β reduced.)

If there were no disturbances in the system, this measurement would provide all of the information about the system trajectory (in the single-state delayed-oscillator model), and thus would be adequate to control the system dynamics. In the presence of disturbances, then in addition, and motivated by the delayed-oscillator description in figure 3, the strength of the Kelvin wave in the central Pacific is also used. This provides advance information about all of the additional disturbances acting on the system before they reach the eastern Pacific, allowing a counteracting influence to be triggered to cancel the effect of the disturbance.

The SST measurement is fed back with a constant gain G. A nonlinear adaptive feedforward approach is used to incorporate the Kelvin wave information, with a filtered-X LMS algorithm identical to that standard in active noise control (Widrow and Stearns 1985). The Kelvin wave is filtered to obtain the desired control signal that will cancel it, with the filter adjusted in real time to minimize the performance (Niño-3 index); in this way, the control adapts automatically to uncertain response characteristics.

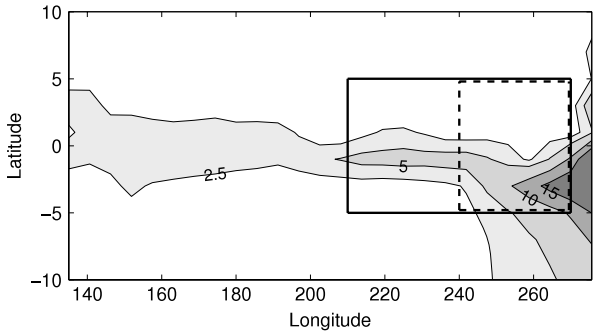

Figure 4. Optimal distribution of forcing; change in Niño-3 index for a change in solar radiation over one grid cell (2° × 5.625°) for excitation at a four year period. The Niño-3 region is shown boxed, the forcing region used is shown with dashed lines.

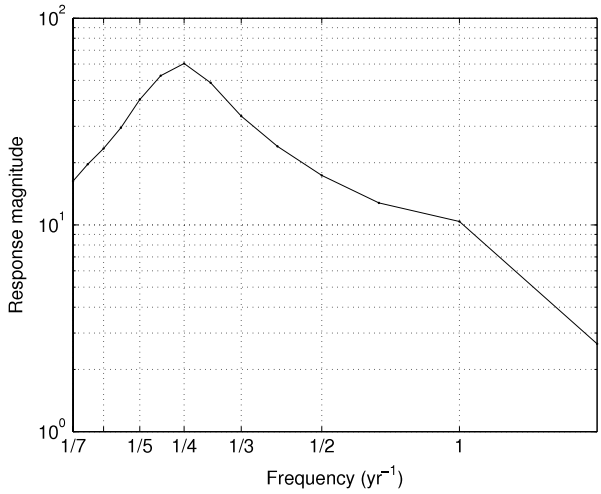

Figure 5. Niño-3 index response to solar forcing, expressed in degrees C per fraction of solar heating over the forcing region (i.e., at a frequency of one cycle per four years, Niño-3 response is slightly more than 1 °C per 2% modulation of solar flux).

With u as the input signal (heating over the eastern half of the Niño-3 region) and y_n and y_k as the measured variables (Niño-3 index and Kelvin wave amplitude), then at each month k

$$u(k) = Gy_n(k) + \sum_{j=0}^{M} w_j(k)x(k-j) \tag{4}$$

where x is obtained by filtering y_k through an estimate of the transfer function between $u(k)$ and the performance $y_n(k)$ (from figure 5), and the filter weights $w_j(k)$ are updated based on a gradient descent algorithm to minimize the mean-square performance:

$$w_j(k+1) = w_j(k) + \mu x(k-j)y_n(k-j) \tag{5}$$

with a step size along the gradient of $\mu < 2(M\langle x^2\rangle)^{-1}$ for stability. The weights converge such that the residual performance y_n under the influence of control is uncorrelated with the filtered reference signal x. Simulations use $M = 6$ since Kelvin wave information older than six months is not useful.

In simulations used to reduce the amplitude of ENSO, the heating perturbation is only allowed to be negative (increasing cloud albedo to reduce heating). Because it is the peak positive excursions in eastern-Pacific SST that are of concern and not the La Niña phase of the oscillation, including this constraint does not significantly affect the simulated performance. In order to enhance the ENSO cycle, positive heating perturbations are useful for maximum effectiveness; in implementation, this would clearly require perturbations about a mean reduction in surface insolation. This is still plausible if increased albedo is being used to offset anthropogenic warming.

4. Simulation

We use the intermediate complexity coupled atmosphere–ocean Cane–Zebiak model of the tropical Pacific, which computes perturbations about a specified monthly climatology with a single layer atmosphere and 1.5 layer ocean. The discretization yields roughly 33 000 state variables. Stochastic mid-Pacific atmospheric wind disturbances are added (from 163° to 197°E and −5° to +5°). With the nominal parameters used in ZC, the system is unstable, and higher than realistic ENSO amplitudes are obtained even with very small disturbance amplitudes (Niño-3 exceeds 2 °C 12% of the time, versus 4.5% actual between 1960 and 2009). Stable ENSO dynamics are obtained by reducing the atmosphere–ocean drag coefficient R^* from 1.0 to 0.8, and much larger disturbance amplitudes are used to produce realistic amplitudes. In all simulations, the automatic atmosphere restarts in the ZC code are monitored to ensure that the solution does not get 'stuck' in non-physical states.

The model is most sensitive to input forcing with a period of four years (see figure 5). Forcing the system with this excitation at each location yields the spatial distribution of forcing effectiveness shown in figure 4. Part of the relative effectiveness is due to the shallower mixed layer depth in the east, so that smaller changes in radiation are needed to produce a change in the temperature of the mixed layer. This confirms the eastern Pacific as the most effective location to force the system with perturbations to the incoming radiation; the remaining simulations use forcing over the eastern half of the Niño-3 region only (120°W–90°W).

Design of feedback control requires some input/output information about the system. The input/output behaviour is plotted in figure 5 for the stable regime of the ZC model, obtained by forcing the model at different frequencies and at small amplitude with no additional disturbances, and with the background climatology replaced by the annual mean to avoid phase-locking with the seasonal cycle (the seasonal cycle is retained in all control simulations). The response (in this stable regime) is essentially that of a damped oscillator. A constant feedback gain of −0.02 gives loop gain greater than one near the ENSO resonant frequency, and excellent stability margins.

MacMynowski and Tziperman (2008) provide an algorithm for estimating the frequency and damping of the dominant ENSO eigenvalue from simulation, without having to construct the linearization. Figure 6 plots the complex eigenvalue

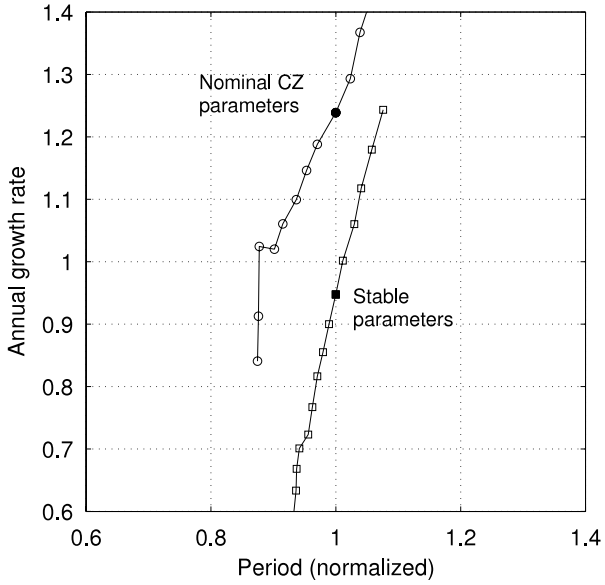

Figure 6. Dominant ENSO eigenvalue dependence on feedback gain, nominal parameters (circles) and stable regime (squares). Zero feedback gain is shown solid. The period is normalized by the nominal period in order to emphasize the relative change in growth rate and period. The irregularity in the eigenvalue trajectory for stabilizing the nominal case is due to phase-locking to the seasonal cycle.

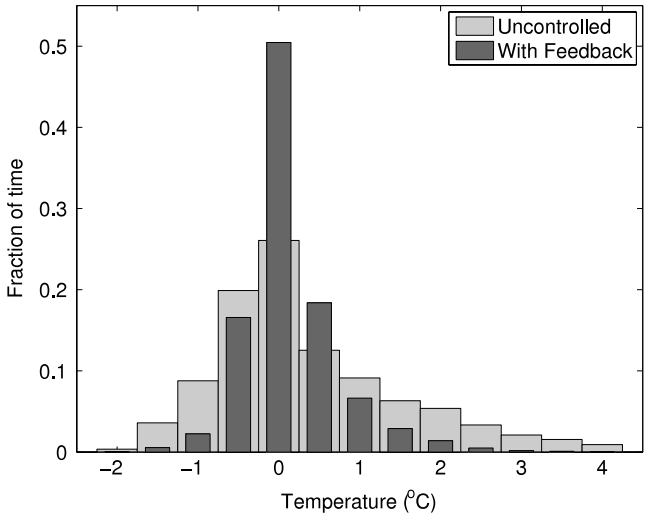

Figure 7. Shift in Niño-3 probability distribution with negative feedback, nominal ZC parameters.

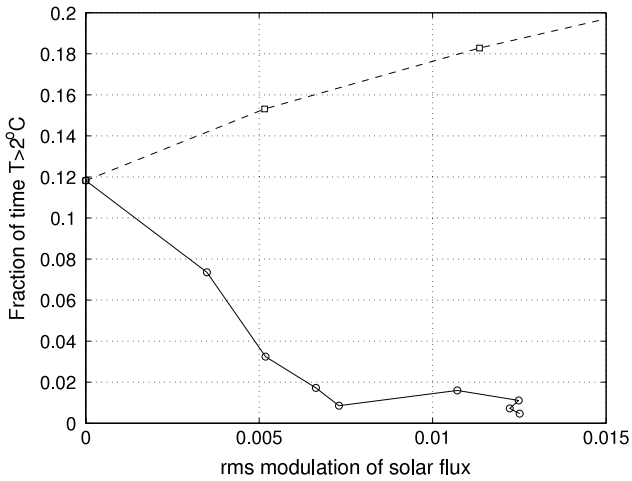

Figure 8. Trade-off between control effort and reduction (or increase) in large ($T > 2\,°\mathrm{C}$) ENSO events with negative (or positive; dashed) feedback, using nominal ZC parameters. Each point corresponds to an increased gain; the last three points (in reducing ENSO amplitude) also use feedforward control.

λ of the annualized discrete-time model ($|\lambda| < 1$ is stable). For either parameter regime considered, the feedback is stabilizing (or destabilizing) with relatively small impact on frequency, as desired.

Feedforward control has the potential to further reduce the response to disturbances by providing information about them in advance. Not surprisingly, in the chaotic regime with the nominal parameters, the addition of feedforward is not necessary because the external disturbances are already small. However, there is relatively little added benefit in the stable regime for the ZC model as well. This is because time delay is not a significant issue with the feedback, and so advance information about the disturbances is not of significant value, especially when the correlation is relatively low.

For the nominal parameters, figure 7 shows the shift in the histogram of Niño-3 indices over a 1000 year simulation with and without feedback control. The fraction of time that Niño-3 exceeds 2 °C drops from nearly 12% to less than 1% of the time while using less than 1% feedback modulation of the solar radiation. (This is about 10 TW of power, substantially more than the 100 GW of power involved in the ocean APE, due to the inefficiency of influencing ocean currents through the surface temperature's impact on winds.) The trade-off between these two metrics as a function of control gain G is shown in figure 8 for nominal parameters and figure 9 for the stable regime. Not surprisingly, the control authority required in the latter case is a factor of a few higher for comparable effect. These figures also illustrate the use of positive feedback to enhance the ENSO cycle.

Turning the feedback off returns the system to its uncontrolled dynamic characteristics; at least in this model, there are no irreversible switches into a different regime.

5. Concluding remarks

A plausible strategy is illustrated to intentionally influence the dynamics of ENSO in order to reduce (or enhance) the probability of extreme El Niño events. The scale of intervention required is quite small if the dynamics are unstable and the observed behaviour is at least partially the result of self-sustained chaotic dynamics. This illustrates a generic result that unstable/chaotic systems can be modified with relatively small energy inputs by using an appropriately designed dynamic feedback approach. Even in the situation where ENSO is a stable system driven by stochastic forcing, the potential to influence its dynamics exists. The forcing required is of a scale achievable by human intervention, and seems plausible if cloud albedo modification were being used to offset some global warming. The quantitative

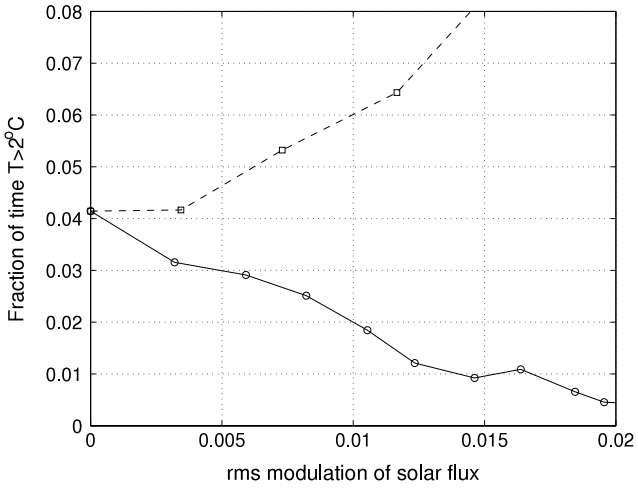

Figure 9. Trade-off between control effort and reduction (or increase) in large ENSO events with negative (or positive; dashed) feedback, for stable regime. Combined feedforward/feedback control is used in reducing ENSO amplitude.

improvements predicted herein will of course depend on the model, nonetheless the general conclusion is still valid.

The ability to influence ENSO does not mean that it is a good idea to do so, though it could be an option if we discover that climate change results in significant changes to the intensity of the cycle.

The strategy proposed herein is not optimal, and an optimized approach would result in using less power for a given change in ENSO amplitude. However, this strategy is plausibly implementable in terms of (i) understanding the physical mechanism that could be used to influence ENSO, and what information to measure, (ii) the feasibility of the power requirements, and (iii) the required understanding of the dynamics (the strategy does not rely on precise prediction of dynamic evolution).

Acknowledgment

The ocean data used is provided by the TAO Project Office of NOAA/PMEL.

References

Bewley T R, Moin P and Temam R 2001 DNS based predictive control of turbulence: an optimal benchmark for feedback algorithms *J. Fluid Mech.* **447** 179–225

Boulanger J-P and Menkes C 1999 Long equatorial wave reflection in the Pacific ocean from TOPEX/POSEIDON data during the 1992–1998 period *Clim. Dyn.* **15** 205–25

Brown J N and Fedorov A V 2008 Mean energy balance in the tropical Pacific ocean *J. Mar. Res.* **66** 1–23

Cane M A 2005 The evolution of El Niño, past and future *Earth Planet. Sci. Lett.* **230** 227–40

Chen D, Cane M A, Kaplan A, Zebiak S E and Huang D J 2004 Predictability of El Niño over the past 148 years *Nature* **428** 733–6

de Boyer Montégut C, Madec G, Fischer A S, Lazar A and Iudicone D 2004 Mixed layer depth over the global ocean: an examination of profile data and a profile-based climatology *J. Geophys. Res.* **109** C12003

Fedorov A V 2007 Net energy dissipation rates in the tropical ocean and ENSO dynamics *J. Clim.* **20** 1108–17

Goddard L and Philander S G 2000 The energetics of El Niño and La Niña *J. Clim.* **13** 1496–516

Hoffman R N 2002 Controlling the global weather *AMS Bull.* **83** 241–8

Joe W T, Taira K, Colonius T and MacMynowski D G 2009 Optimized control of vortex shedding from an inclined flat plate *AIAA Paper 2009-4027*

Keith D 2000 Geoengineering the climate: history and prospect *Annu. Rev. Energy Environ.* **25** 245–84

Latham J 2002 Amelioration of global warming by controlled enhancement of the albedo and longevity of low-level maritime clouds *Atmos. Sci. Lett.* **3** 52–8

Latham J, Rasch P, Chen C-C J, Kettles L, Gadian A, Gettelman A, Morrison H, Bower K and Choularton T 2008 Global temperature stabilization via controlled albedo enhancement of low-level maritime clouds *Phil. Trans. R. Soc.* A **366** 3969–87

MacMynowski D G and Tziperman E 2008 Factors affecting ENSO's period *J. Atmos. Sci.* **65** 1570–86

McPhaden M *et al* 1998 The tropical ocean-global atmosphere (TOGA) observing system: a decade of progress *J. Geophys. Res.* **103** 169–240

Penland C and Sardeshmukh P D 1995 The optimal-growth of tropical sea-surface temperature anomalies *J. Clim.* **8** 1999–2024

Philander S G and Fedorov A 2003 Is El Niño sporadic or cyclic? *Annu. Rev. Earth Planet. Sci.* **31** 579–94

Schneider S H 1996 Geoengineering: could or should we do it? *Clim. Change* **33** 291–302

Suarez M J and Schopf P S 1988 A delayed action oscillator for ENSO *J. Atmos. Sci.* **45** 3283–7

Tziperman E, Scher H, Zebiak S E and Cane M A 1997 Controlling spatiotemporal chaos in a realistic El Niño prediction model *Phys. Rev. Lett.* **79** 1034–7

Tziperman E, Stone L, Cane M A and Jarosh H 1994 El-Niño chaos: overlapping of resonances between the seasonal cycle and the Pacific ocean-atmosphere oscillator *Science* **264** 72–4

Van Oldenborgh G J, Burgers G, Venzke S, Eckert C and Giering R 1999 Tracking down the ENSO delayed oscillator with an adjoint OGCM *Mon. Weath. Rev.* **127** 1477–95

Wei M J and Freund J B 2006 A noise-controlled free shear flow *J. Fluid Mech.* **546** 123–52

Widrow B and Stearns S D 1985 *Adaptive Signal Processing* (Englewood Cliffs, NJ: Prentice-Hall)

Yeh S-W, Kug J-S, Dewitte B, Kwon M-H, Kirtman B P and Jin F-F 2009 El Niño in a changing climate *Nature* **461** 511–4

Zebiak S E and Cane M A 1987 A model El Niño-Southern Oscillation *Mon. Weath. Rev.* **115** 2262–78